Cellulose (2023) 30:6457–6469
https://doi.org/10.1007/s10570-023-05288-4

ORIGINAL RESEARCH

A nitrocellulose/cotton fiber hybrid composite membrane for paper-based biosensor

Ruihua Tang · Mingyue Xie · Xueyan Yan · Liwei Qian · John P. Giesy · Yuwei Xie

Received: 19 January 2023 / Accepted: 24 May 2023 / Published online: 3 June 2023

Abstract Nitrocellulose (NC) membrane was fabricated and tested for its potential use in various paper-based biosensors for use in point-of-care testing. However, contemporary technologies are complex, expensive, non-scalable, limited by conditions, and beset with potentially adverse effects on the environment. Herein, we proposed a simple, cost-effective, scalable technology to prepare nitrocellulose/cotton fiber (NC/CF) composite membranes. The NC/CF composite membranes with a diameter of 20 cm were fabricated in 15 min using papermaking technology, which contributes to scalability in the large-scale production of these composites. Compared with existing commercial NC membranes, the NC/CF composite membrane is characterized by small pore size (3.59 ± 0.19 μm), low flow rate (156 ± 55 s/40 mm), high dry strength (up to 4.04 MPa), and wet strength (up to 0.13 MPa), adjustable hydrophilic-hydrophobic (contact angles ranged from 29 ± 4.6 to $82.8 \pm 2.4°$), the good adsorption capacity of protein (up to 91.92 ± 0.07 μg). After lateral flow assays (LFAs) detection, the limit of detection is 1 nM, which is similar to commercial NC membrane (Sartorius CN 140). We envision the NC/CF composite membrane as a promising material for paper-based biosensors of point-of-care testing applications.

Keywords Nitrocellulose · Cotton fiber · Point-of-care testing · Papermaking technology · Lateral flow assays

R. Tang (✉) · M. Xie · X. Yan · L. Qian
College of Bioresources Chemical and Materials Engineering, Shaanxi University of Science and Technology, Xi'an 710021, People's Republic of China
e-mail: tangruihua@163.com

R. Tang · M. Xie · X. Yan · L. Qian
National Demonstration Center for Experimental Light Chemistry Engineering Education, Shaanxi University of Science and Technology, Xi'an 710021, People's Republic of China

J. P. Giesy
Toxicology Center, University of Saskatchewan, 44 Campus Dr, Saskatoon S7N 5B3, Saskatchewan, Canada

J. P. Giesy
Department of Veterinary Biomedical Sciences, University of Saskatchewan, Saskatoon, SK S7N 5B4, Canada

J. P. Giesy
Department of Integrative Biology and Center for Integrative Toxicology, Michigan State University, East Lansing, MI 48824, USA

J. P. Giesy
Department of Environmental Science, Baylor University, One Bear Place #97266, Waco, TX 76798-7266, USA

Y. Xie
Ministry of Ecology and Environment, Nanjing Institute of Environmental Sciences, Nanjing 210042, China

Introduction

Green/sustainable cellulose paper-based biosensors have received considerable interest in vitro diagnostics in resource-limited settings due to its cost-effective, simple to operate, portable, and rapid as compared to these high-cost and long analysis time traditional methods (e.g., quantitative real-time polymerase chain reaction, enzyme-linked immunosorbent assays) (Liu et al. 2021b; Xiao et al. 2022). The paper-based biosensors have been extensively used for rapid tests supporting public health, environmental monitoring, and food safety monitoring (Fan et al. 2020; Modha et al. 2021; Noviana et al. 2021). Diagnostic biosensors have been developed in response to the COVID-19 pandemic (Tang et al. 2021), circulation of Salmonella typhimurium, *Escherichia coli* O157:H7 (Zheng et al. 2021) and alpha-fetoprotein, and carcinoembryonic antigen (Lin et al. 2022). Lateral flow assays (LFAs) (Ince et al. 2022; Sena-Torralba et al. 2022), vertical flow assays (VFAs) (Bhardwaj et al. 2019; Chen et al. 2020), ELISAs (Charernchai et al. 2022; Dignan et al. 2021), cell-based biosensors (Liu et al. 2021a), and wearable sensors (Gao et al. 2019a) are popular biosensors at point-of-care testing (POCT). Due to their high capability of binding proteins, hydrophilicity, and flexibility, nitrocellulose (NC) membranes as a porous substrate play an important role in developing paper-based biosensors (Tang et al. 2022b).

Several technologies have been developed to prepare NC membranes, including phase inversion (Khamis et al. 2020), electrospinning (Wang et al. 2020), and spin coating (Horstmann et al. 2020). Phase conversion technology requires complex post-treatment operation after casting nitrocellulose solution onto glass plates to NC membrane with high porosity and tunable pore size, requiring 17 h (Ahmad et al. 2008; Khamis et al. 2020; Tang et al. 2019b). Electrospinning technology relying on a strong electric field is limited by relatively poor yields and costs of equipment, needing 36 h (B. Naderizadeh et al. 2012; Luo et al. 2012; Wang et al. 2020). Spin coating technology utilizes centrifugal forces to disperse polymer solution on a flat polyester film substratum to reproducibly prepare NC membranes of uniform structure, requiring 13.5 h (Wang et al. 2022b; Yin et al. 2010). In contrast, this technology only uses a small and flat substrate and uses large amounts of solution during operation, which makes it unsuitable for large-scale manufacture. Besides that, these technologies all still need toxic solvents to dissolve nitrocellulose and are time-consuming (> 12 h) to dissolve, defoam, and dry. Additionally, these NC membranes fabricated by the above technologies often used plastic substrate (e.g., Commercial polyester transparent film (Pawar et al. 2019)) to improve their mechanical strength for achieving paper-based biosensor detection. Thus, these technologies are complex, expensive, limited by their specific conditions and not amenable for large-scale production, and are unfriendly environments. Therefore, there is a demand for a simple, cost-effective technology that can be used on a large scale to prepare NC membranes that are uniform and provide good performance.

Traditional papermaking technology is simple, low-cost, and can prepare large volumes of various films (Cao et al. 2021; Huang et al. 2021; Liao et al. 2022), and offers an opportunity to develop simple, cost-effective, large-scale, methods to prepare high-performance composite paper-based materials. Cellulose/phenol–formaldehyde resin composite film with strong mechanical properties of 140 MPa tensile strength, excellent robustness, and broadband light management (high transparency (~86%), optical haze (~90%) and excellent anti-ultraviolet performance) has been fabricated (Sun et al. 2021). Aramid nanofibers/polyphenylene sulfide composite membranes with excellent thermal stability, flame-retardancy, better interfacial compatibility, and ion conductivity (1.43 mS cm^{-1}) have been prepared and used as separators in lithium-ion batteries (Zhu et al. 2019). Recently, carbon fiber/graphene oxide/cellulose composite paper electrodes with well-controlled structure, flexibility, stability, and repeatability have been developed for phenol electrochemical detection (Wang et al. 2022a). Based on the above analysis, papermaking technology is suitable for the scalable production of composite materials. In addition, cotton fiber has been used to mix with other materials to fabricate composite material with high mechanical strength (Seki et al. 2022). However, the application of papermaking technology for nitrocellulose/cotton fiber (NC/CF) composite membranes preparation of paper-based biosensors has been rare.

Here, we proposed a simple, low-cost, effective, and large-scale papermaking technology to prepare NC/CF composite membranes. This NC/

CF composite membrane was fabricated by NC and CF. Next, its physical properties, including porous structure, hydrophilicity, flow rate, and mechanical strength, and chemical properties, including surface elements, functional groups, crystal structure, and protein adsorption capacity, were characterized. Finally, human immunodeficiency virus (HIV) and LFAs were utilized to validate the performance.

Experimental section

Chemicals and materials

Cotton pulp was acquired from Hubei Jinhuan New Material Technology Co., Ltd. (Hubei, China). Nitrocellulose (NC) of H 1/2 type with 11.5–12.2% nitrogen content was supplied by Hengshui Heshuo Cellulose Co., Ltd. (Hebei, China). HIV probe (HIV capture probe, HIV control probe, and HIV detection probe), target DNA, and 20 × SSC buffer was obtained from Sangon Biotech Co., Ltd. (Shanghai, China). Streptavidin was purchased from Promega Corporation (USA). Sodium phosphate tribasic ($Na_3PO_4{\cdot}H_2O$), sodium dodecyl sulfate (SDS), sodium chloride (NaCl), and sugar were obtained from Damao Chemical Reagent Factory (Tianjin, China). Phosphate buffer saline (PBS), albumin bovine (full component), and 5 × Coomassie brilliant blue G-250 solution were obtained from Solarbio Co., Ltd. (Beijing, China). Commercial NC (CNC) membrane (Sartorius CN 140), absorbent pad, conjugation pad, sample pad, and backing pad were bought from Jiening Biotech Co., Ltd. (Shanghai, China). All chemical reagents were of analytical purity.

Preparation of NC/CF composite membrane

NC/CF composite membranes with 80 g/m^2 basis weight were fabricated by the papermaking process (Fig. 1). First, various ratios of NC and CF (1:9, 1:1, and 9:1) were mixed and dispersed by a standard slurry dispenser, then, the mixed solutions were transferred to the paper former. Next, all mixed solutions were filtrated under vacuum to fabricate different wet NC/CF composite membranes. Finally, these wet NC/CF composite membranes were dried to generate various NC/CF composite membranes with a diameter of 20 cm, which were named 10% NC/CF composite membranes, 50% NC/CF composite membranes, and 90% NC/CF composite membranes, respectively.

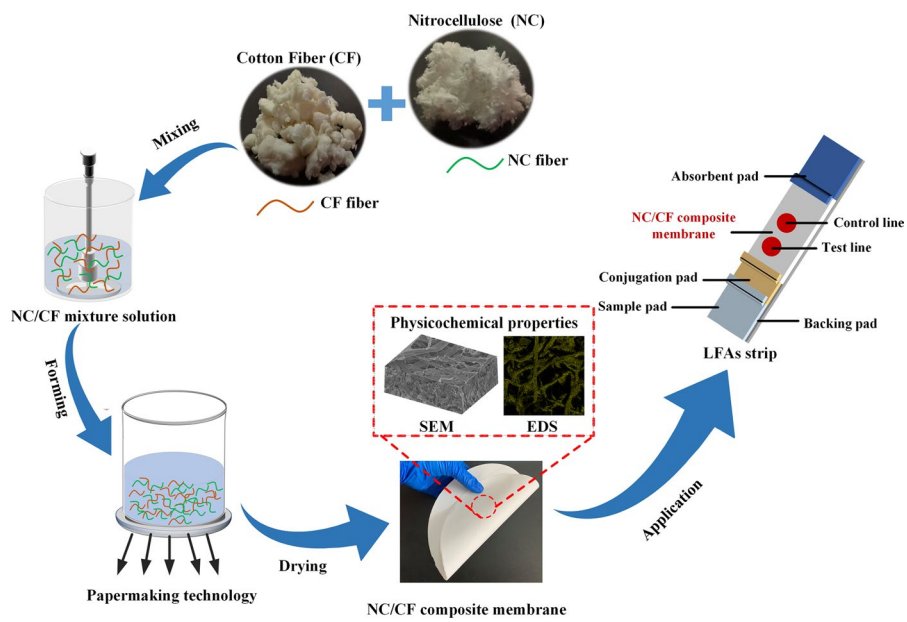

Fig. 1 Schematic of the preparation process of NC/CF composite membrane by papermaking technology and its application for HIV LFAs

Characterizations of physicochemical properties of the NC/CF composite membranes

The thickness of these NC/CF composite membranes was measured by the digital thickness gauge (Xinyuan Hengtong Household Products Co., Ltd., China), and the basis weight and tightness of these NC/CF composite membranes were calculated according to previously reported literature (Tang et al. 2022a). Scanning electron microscopy (SEM) (VEGA-3-SBH, TESCAN, Czech Republic) was used to observe the front and cross-sectional morphologies of different NC/CF composite membranes after being coated with gold, and then the pore size and porosity of these NC/CF composite membranes were evaluated by mercury porosimeter (Auto Pore IV 9500, Micromeritics, USA). Flow rates of NC/CF composite membranes were detected according to the reported literature with slight modification (Ahmad et al. 2007). The detailed process was as follows: these NC/CF composite membranes were cut into strips with 15 mm × 40 mm (width × length), the strip was immersed in deionized water and the time was measured from start point to end point in the vertical direction. Finally, the flow rate was calculated by the length/the time. The dry tensile strength and wet tensile strength (immersing the sample in water for 20 min) of these NC/CF composite membranes were measured by Servo material multifunctional high and low-temperature control testing machine (AI-7000-NGD, Goodtechwill, China) according to the reported literature with slight modification (Liu et al. 2023). In detail, these NC/CF composite membranes were cut into 40 mm × 10 mm (length × width), and the tensile speed of samples was 1 mm/min. Meanwhile, NC/CF composite membranes were first cut into circles with a diameter of 6 mm by punching and then immersed in deionized water for 0 min or 20 min. Changes in the shape of these NC/CF composite membranes were observed by images with the smartphone (Huawei nova 6). The hydrophilicity of these NC/CF composite membranes were evaluated by dynamic absorption contact angle (DAT1100, Fibro, Sweden).

Surface elements, surface functional groups, and crystal structures of different NC/CF composite membranes were measured by energy-dispersive x-ray spectroscopy (EDS) (VEGA-3-SBH, TESCAN, Czech Republic), Fourier transform infrared (FT-IR) (Vertex 70, Netzsch, Germany) and X-ray diffractometer (XRD) (Bruker, D8 Advance, Germany). For EDS, the elemental species and content of these NC/CF composite membrane surfaces at 1000 × were obtained using the face scan mode. For FT-IR, these NC/CF composite membranes were cut into small pieces and mixed with dried potassium bromide (KBr) powder, and the mixture was then pressed into tablets. Transmission mode measurements were carried out at a resolution of 4 cm^{-1} over the spectral range of 500 to 4000 cm^{-1}. For XRD, NC fiber or the mixture of NC fiber and CF fiber were placed uniformly and flatly on the sample table, the scanning speed was 6°/min, the scanning step was 0.02° and the scanning range was 5 to 60°. Capacity to absorb the protein of these NC/CF composite membranes was measured according to the reported literature with slight modification (Sun et al. 2007; Tang et al. 2020). BSA was chosen as a model of protein adsorption. First, NC/CF composite membrane was cut into 1 cm × 1 cm. Next, six sheets of NC/CF composite membrane were incubated and shaken in 2 mL of BSA solution with 1 mg/mL for 3 h at room temperature. After adsorption, the optical densities of residual BSA solutions were measured by a multifunctional microplate reader (Thermo Scientific, Germany) at 595 nm according to the Bradford method. The concentration of BSA was calculated according to the standard curve. Then, the volumes of residual BSA solutions were examined by pipette. Finally, the adsorption capacity of BSA on these NC/CF composite membranes was calculated by the equation (The adsorption capacity of protein = Initial concentration of BSA × initial volume -Residual concentration of BSA × residual volume.

LFAs detection

Gold nanoparticles (AuNPs) with a diameter of 13 nm were prepared as previously described (Hu et al. 2013). HIV as the model target, these sequences of the control probe, capture probe, and detection probe were synthesized according to the reported literature (Tang et al. 2016). First, the sample pad, conjugation pad, NC/CF composite membrane, and absorbent pad were assembled sequentially on the backing pad. Then, it was cut into LFAs strips of width and length of 4 and 60 mm, respectively using a ZQ2000 rapid test cutter. Then, the control probe and capture probe were added to the NC/CF composite membrane, and

gold nanoparticles modification with the detection probe were added on the conjugation pad, respectively. Next, it was dried in the oven at 37 °C for 2 h. 100 µL of different concentrations of HIV target (50 nM, 25 nM, 10 nM, 5 nM, 2.5 nM, 1 nM, 0.5 nM, 0.25 nM, and 0 nM) were detected. Finally, the images were collected by Huawei nova 6, and the optical density was measured by IPP6.0 software. All experiments were repeated with three replicates.

Results and discussion

To address limitations associated with existing NC membranes, a simple, low-cost, large-scalable (operation time: 15 min), and high-performance papermaking technology was developed to prepare NC/CF composite membrane (Fig. 1). The basic physical and chemical properties of the NC/CF composite membrane including porous structure, hydrophilicity, flow rate, mechanical strength, surface elements, functional groups, crystal structure, and protein adsorption capacity were firstly investigated. Then, we chose LFAs as a paper-based POCT platform to demonstrate its application performance.

Physicochemical properties of NC/CF composite membrane

To understand the physical properties of pure CF membranes and NC/CF composite membranes, the thickness, basis weight, and tightness of these materials were measured (Table 1). The thickness of these materials was pure CF membrane < 10% NC/CF composite membrane < 50% NC/CF composite membrane < 90% NC/CF composite membrane because the binding ability of hydroxyl groups between the fibers was inversely proportional to the content of NC. The basis weight and tightness of these materials was pure CF membrane > 10% NC/CF composite membrane > 50% NC/CF composite membrane > 90% NC/CF composite membrane because the binding ability of hydroxyl groups between the fibers was inversely proportional to the content of NC. All these results are well supported by the introduction of cotton fiber to improve the binding ability of NC fibers. Based on the above analysis, morphologies of these NC/CF composite membranes containing various contents of NC were characterized. The morphologies indicated that cellulose fiber and NC fiber intertwined to form their porous structure (Fig. 2A). **T**he result of the front section indicated that the pore size of these pure CF membranes and NC/CF composite membranes with different NC contents was 90% NC/CF composite membrane (5.96 ± 1.15 µm) > 50% NC/CF composite membrane (5.41 ± 1.07 µm) > 10% NC/CF composite membrane (3.59 ± 0.19 µm) > pure CF membrane (2.35 ± 0.22 µm) (Fig. 2A (a_1, a_2, a_3, a_4)). These results indicated that the pore size of 10% NC/CF composite was smallest in the NC/CF composite membranes (Fig. 2B) since the cotton fiber of 10% NC/CF composite membrane was higher than other NC/CF composite membranes, and more hydroxyl groups enhanced the bonding between fibers. The result that the porosity of the NC/CF composite membrane was increased from 77.74 ± 0.008% (pure CF membrane) to 87.54 ± 0.43% (90% NC/CF composite membrane) (Fig. 2B), indicating that the adsorption capability of water of the NC/CF composite membrane increased with the increase of porosity. The result of the cross-section showed that the thickness of these NC/CF composite membranes was similar to the trend of the above thickness measurements (Fig. 2A (b_1, b_2, b_3, b_4)). In addition, flow rates of these NC/CF composite membranes were also investigated (Fig. 2C). Flow rates through these NC/CF composite membranes is 50% NC/CF composite membrane (68.33 ± 21.22 s/40 mm) > 90% NC/CF composite membrane (146.67 ± 35.12 s/40 mm) > 10% NC/CF composite membrane (156.33 ± 55.82 s/40 mm) > pure CF membrane (231 ± 29.20 s/40 mm), which demonstrated

Table 1 The basic physical properties of pure CF membranes and NC/CF composite membranes

Sample	Thickness (mm)	Basis weight (g/m^2)	Tightness (g/cm^3)
CF membrane	0.22 ± 0.02	78.13 ± 0.07	0.35 ± 0.004
10% NC/CF composite membranes	0.23 ± 0.03	77.81 ± 0.06	0.33 ± 0.002
50% NC/CF composite membranes	0.25 ± 0.02	74.34 ± 0.06	0.30 ± 0.004
90% NC/CF composite membranes	0.26 ± 0.04	72.66 ± 0.09	0.27 ± 0.002

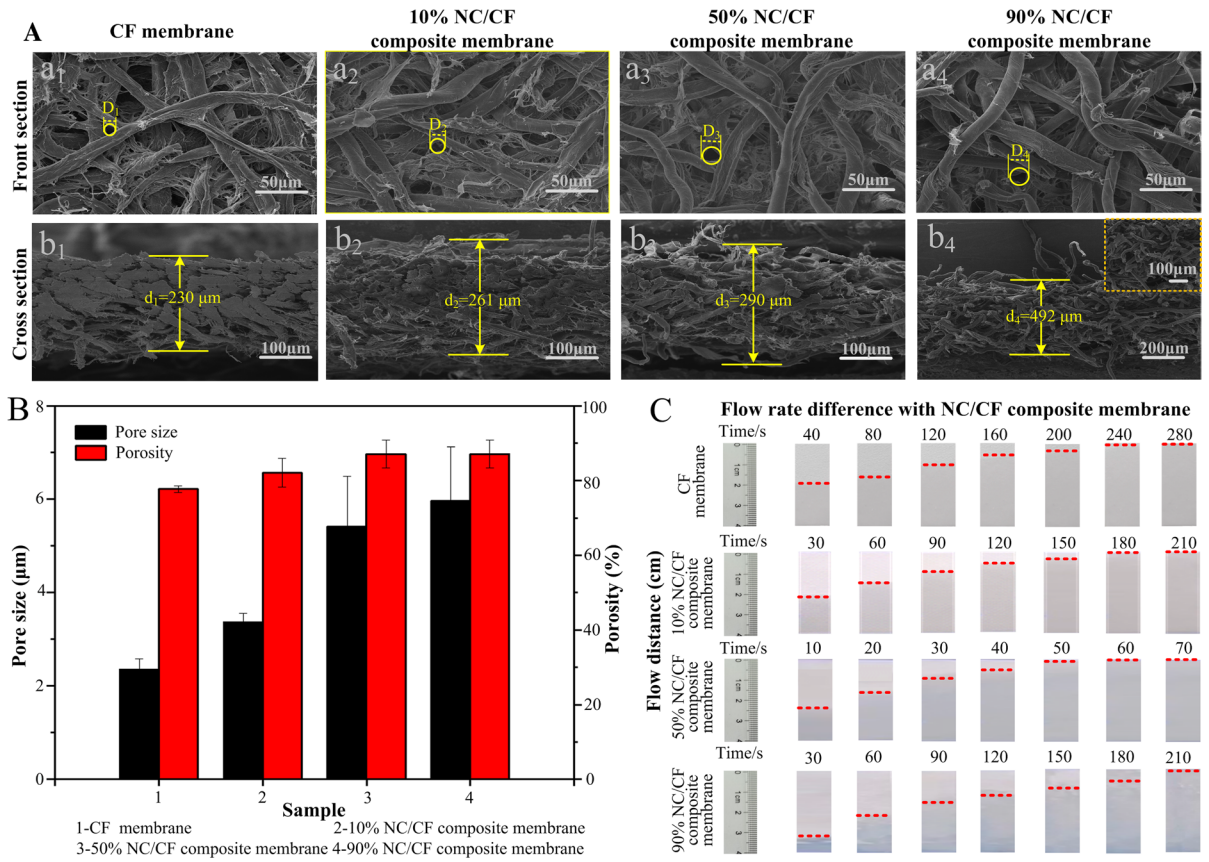

Fig. 2 The physical properties of these pure CF membranes and NC/CF composite membranes. **A** The morphology of these pure CF membranes and NC/CF composite membranes, including front section **a** and cross section **b**. **B** The pore size, porosity of these pure CF membranes and NC/CF composite membranes. **C** The flow rate of these pure CF membranes and NC/CF composite membranes

that the flow rate of 10% NC/CF composite membrane was slowest in the NC/CF composite membranes. Larger flow resistance in the NC/CF composite membrane is due to the smaller pore size of 10% NC/CF composite membrane (Low et al. 2013).

Pure CF membranes had higher dry tensile strength (~5.09 MPa) and wet tensile strength (~0.14 MPa) as compared to these NC/CF composite membranes, because the surface of cotton fiber has abundant hydroxyl groups that increase the bonding between cotton fiber. In these NC/CF composite membranes, the dry tensile strength of 10% NC/CF composite membrane was greatest (~4.04 MPa), while that of 90% NC/CF composite membrane was the least (~0.062 MPa) (Fig. 3A). The wet tensile strength of 10% NC/CF composite membrane was greatest (~0.13 MPa), while that of 90% NC/CF composite membrane was the least (~0.015 MPa) (Fig. 3B). It demonstrated that the introduction of CF could enhance the mechanical strength of NC/CF composite membrane because the pure NC fiber could not be fabricated membrane by the papermaking technology. Additionally, the ability of NC/CF membranes to bind hydrogen was inversely proportional to NC content with/without immersion in deionized water. Considering the practical application of the NC/CF composite membrane, the shape changes of the NC/CF composite membrane were further investigated through immersion in water after 20 min. Compared to other NC/CF composite membranes, the edge of 90% NC/CF composite membrane was partially damaged (Fig. 3C), which indicated the hydrogen bonds between these fibers are broken after immersion in water. Additionally, the hydrophilic-hydrophobic

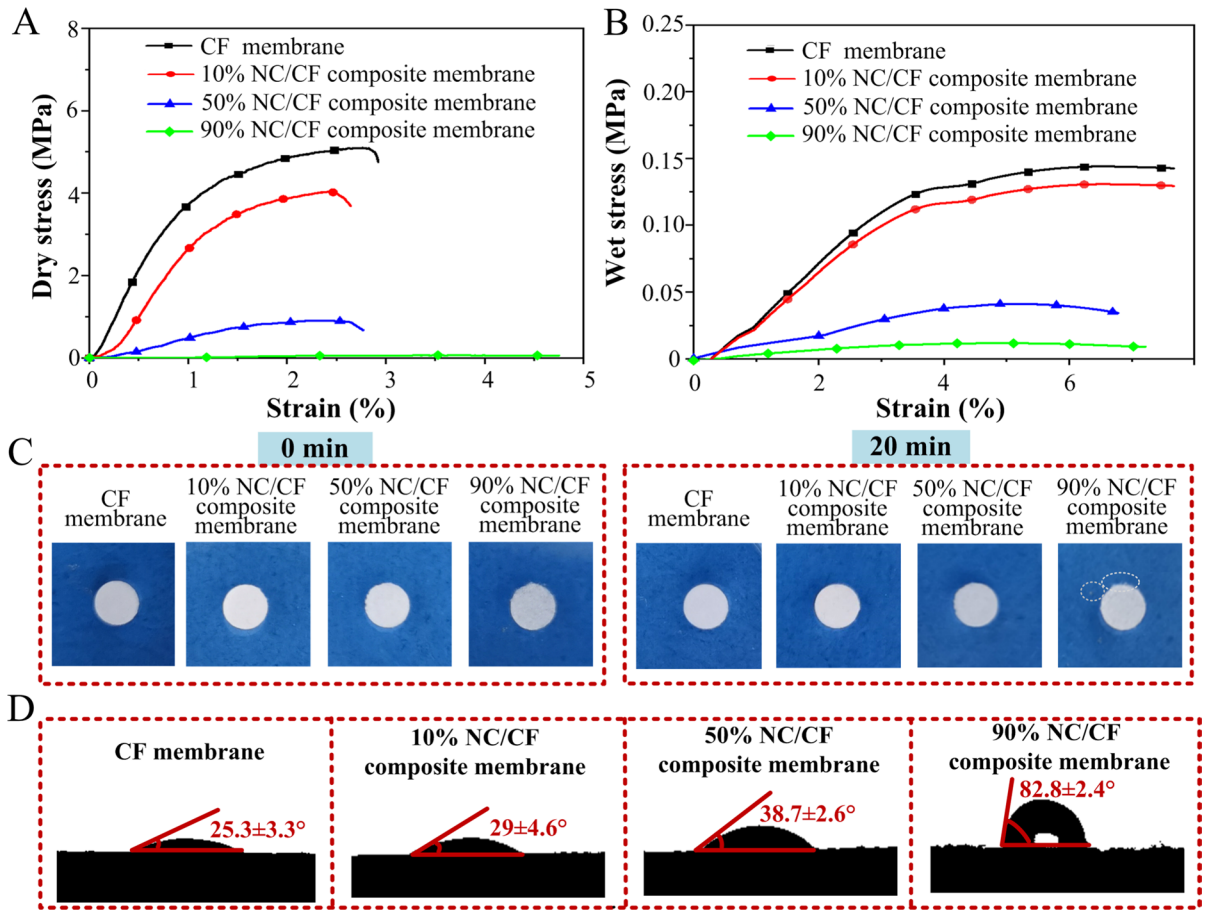

Fig. 3 The physical properties of these pure CF membranes and NC/CF composite membranes. **A** The dry tensile strength of these pure CF membranes and NC/CF composite membranes. **B** The wet tensile strength of these pure CF membranes and NC/CF composite membranes. **C** The shape changes of these pure CF membranes and NC/CF composite membranes before and after immersion in water. **D** The contact angles of these pure CF membranes and NC/CF composite membranes

property was shown, the result that the contact angle of the NC/CF composite membranes was increased from 25.3 ± 3.3 (pure CF membrane) to 82.8 ± 2.4 ° (90% NC/CF composite membrane) (Fig. 3D). Hydrophilicity of these NC/CF composite membranes was inversely proportional to NC content.

NC/CF composite membranes with different NC contents were successfully prepared by the proposed/developed papermaking technology. The surface of pure CF membranes contained C and O elements. The surface of NC/CF composite membranes contained C, O, and N elements, and the content of N of the NC/CF composite membrane was positively correlated with the amount of NC (Fig. 4A). From the FT-IR spectrum, the spectrum of NC/CF composite membrane has all the absorption bands of NC fiber and CF, although some peaks of both structures are overlapping. The basic characteristic peaks of NC/CF composite membrane at 3600–3400 cm^{-1}, 1636 cm^{-1}, and 1273 cm^{-1}, in correspondence to the stretching vibrations of O–H, the asymmetric and symmetrical stretching vibrations of the $–NO_2$, respectively, which agree with the structure of NC (Fig. 4B) (Fernández de la Ossa et al. 2011). It is noted that the $–NO_2$ functional group of the NC/CF composite membrane increased significantly with the increase of NC content, which contributes to enhancing the adsorption of biomolecules of the NC/CF composite membrane because the strong dipole of the $–NO_2$ functional group on the NC/CF composite membrane could interact the

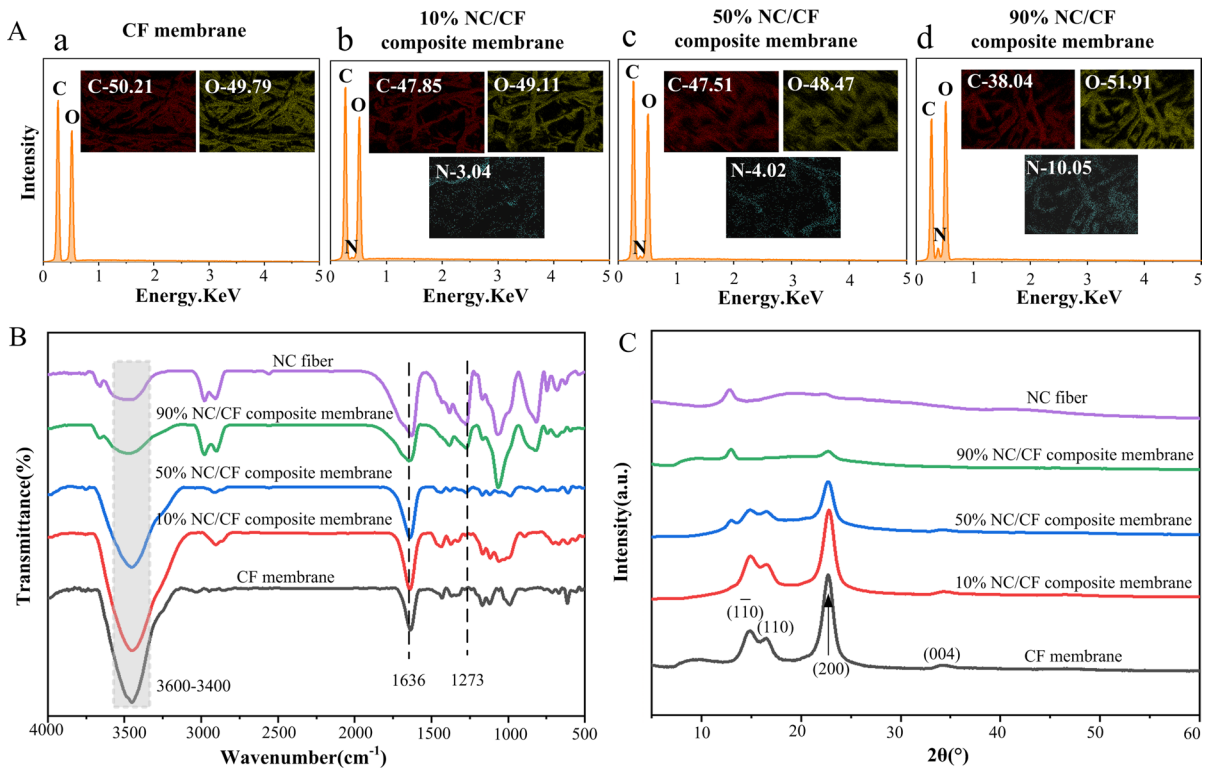

Fig. 4 The chemical properties of these pure CF membranes and NC/CF composite membranes. The result of EDS images **A**, FT-IR spectrum **B** and XRD patterns **C**

high dipole of the peptide bonds on the protein surface via electrostatic forces (Tang et al. 2019a).

Introducing CF can change the crystal structure of the NC/CF composite membrane. The main characteristic diffraction peaks of the NC/CF composite membrane at 2θ = 14.8 °, 16.5 °, 22.8 ° and 34.4 ° (XRD patterns, Fig. 4C), in line with (1–10), (110), (200), (004) crystal planes of cellulose I structure, respectively. In comparison, at 2θ = 12.9°, XRD patterns corresponded to one part of the NC crystalline domain (Sebe et al. 2012; Trache et al. 2016). Furthermore, the characteristic diffraction peak of type cellulose I structure of the NC/CF composite membrane was gradually weakened, and the signal intensity of the NC crystalline domain was gradually increased with the increase of NC content and the decrease of CF.

Finally, the adsorption capacity of biomolecules of material as a key parameter could affect the property of paper-based biosensors. Thus, the adsorption capacity of protein of pure CF membranes and NC/CF composite membrane was also examined (Fig. 5). Capacities of these NC/CF composite membranes to absorb BSA was 10% NC/CF composite membrane (91.92 ± 0.07 μg) > 50% NC/CF composite membrane (60.87 ± 0.1 μg) > 90% NC/CF composite membrane (56.21 ± 0.08 μg) > pure CF membranes (46.22 ± 0.05 μg) (Fig. 5B), indicating that the 10% NC/CF composite membrane has the greatest capacity to absorb protein according to the standard curve of BSA (Fig. 5A). This is because the pore size of other NC/CF composite membranes was too large or too small for biomolecules adsorption (Hartmann et al. 2013). Based on the results of the characterization of the physiochemical properties of NC/CF composite membranes, the 10% NC/CF composite membrane as the optimal membrane was used for LFAs application.

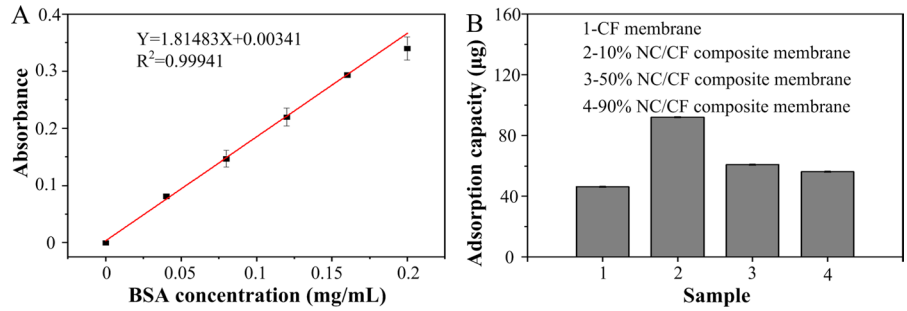

Fig. 5 The adsorption capacity of protein of these pure CF membranes and NC/CF composite membranes. **A** The standard curve of BSA solution. **B** The adsorption capacity of protein of these pure CF membranes and NC/CF composite membranes

Application of LFAs

To further verify the performance of NC/CF composite membrane in a paper-based biosensor, 10% NC/CF composite membrane was used as the substrate was fabricated to LFAs strips (Fig. 6A). The result of HIV target detection illustrated that the detection limit of LFAs of NC/CF composite membrane was 1 nM (Fig. 6B). To further compare the differences between 10% NC/CF composite membrane and existing commercially available membranes, CNC membrane (Sartorius CN 140) was also used to fabricate LFA strips with a detection limit of 1 nM (Fig. 6C). That result verified that both sensitivities were consistent. However, the optical densities of LFAs of 10% NC/CF composite membrane with different sample concentrations were less than that of the CNC membrane (Fig. 6D). To analyze this phenomenon,

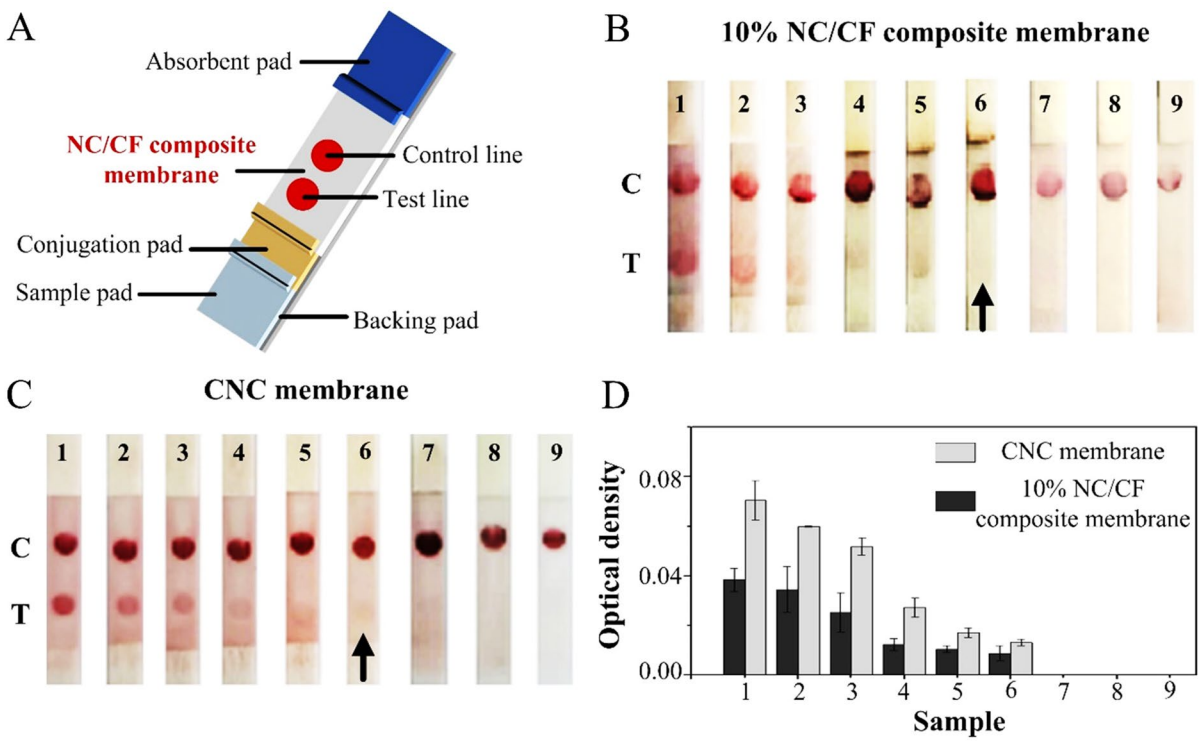

Fig. 6 HIV detection. **A** Schematic of LFAs strip. **B** The detection limit of 10% NC/CF composite membranes was 1 nM. **C** The detection limit of CNC membrane was 1 nM. **D** The optical density of test line on 10% NC/CF composite membranes and CNC membranes

Table 2 Types and properties of some existing commercial NC membranes

NC membrane type	Manufacturer	Pore size	Flow rate	Dry tensile strength	Water contact angle	Protein adsorption capacity	References
Hybridization NC Filter membrane	Millipore	0.45 μm	–	0.18 ± 0.1 MPa	–	21.32%	Sathirapongsasuti et al.(2021)
HF 18002	Millipore	1.08 μm	180 s/4 cm	–	67°	–	Li et al. (2019)
HF 120	Millipore	17 ± 1 μm	42 s/2 cm	–	–	–	Alam et al. (2021)
HFB 18002	Millipore	5.46 μm	180 s/4 cm	–	0°	–	Zhang et al. (2019)
HFC 13502	Millipore	–	135 s/4 cm	–	–	–	Gao et al. (2019b)
HFB 18002	Millipore	–	180 s/4 cm	–	–	–	
HFC 18002	Millipore	–	180 s/4 cm	–	–	–	
Pall vivid 90	Pall	11.87 ± 1.95 μm	80–100 s/4 cm	–	–	–	Tang et al. (2020)
Sartorius CN 95	Sartorius	5.8 ± 0.98 μm	96.9 s/4 cm	–	–	–	Tang et al. (2020)
Sartorius CN 140	Sartorius	3.2 ± 0.85 μm	134.3 s/4 cm	–	–	–	Tang et al. (2020)
Pall vivid 170	Pall	4.22 ± 0.85 μm	50–225 s/4 cm	–	–	–	Tang et al. (2020)
HFB 13500	Millipore	–	135 s/4 cm	–	0°	–	Yew et al. (2018)
Sartorius CN 140	Sartorius	–	60 s/4 cm	–	–	5.04%	Wang et al. (2020)
commercial NC membrane	Shanghai JieYi Biotechnology	–	60 s/4 cm	–	0°	5.3%	Wang et al. (2021)
10% NC/CF composite membrane	This work	3.59 ± 0.19 μm	156 ± 55 s/4 cm	4.04 MPa	29 ± 4.6°	91.92 ± 0.07 μg (11.66%)	This work

the pore size of the CNC membrane and 10% NC/CF composite membrane were compared. The size of pores of the CNC membrane (3.2 ± 0.85 μm) was less than that of the 10% NC/CF composite membrane (3.59 ± 0.19 μm), which indicated that the smaller pore size increased the interaction between biomolecules and further improved the optical density of the CNC membrane test line (Yahaya et al. 2019).

Conclusions

In this study, papermaking technology was successfully applied to develop cost-effective technology and could be used to prepare larger-scale NC/CF composite membranes. Smaller pore size (3.59 ± 0.19 μm), lesser flow rate (156 ± 55 s/40 mm), good mechanical strength (dry tensile strength up to 4.04 MPa and wet tensile strength up to 0.13 MPa), greater hydrophilicity (contact angle up to 29 ± 4.6°) and greater than the adsorption capacity of protein (91.92 ± 0.07 μg) as compared to existing commercial NC membrane (Table 2). For LFAs application, in addition, a 10% NC/CF composite membrane could achieve a similar sensitivity to the commercial membrane (Sartorius CN 140). Hence, we envision that our NC/CF composite membrane has great potential for other paper-based platforms.

Acknowldgments Not applicable.

Author contribution Conception, figure design, writing the original draft and review & editing were performed by RT. Material preparation, data collection, analysis, figure design and writing the original draft were performed by MX and XY. Writing-review & editing was performed by LQ, JP. G and YX. All authors read and approved the final manuscript.

Funding This work was supported by the key research and development Plan of Shaanxi Province (2023-YBSF-154), the Natural Science Research Foundation of Shaanxi University of Science & Technology (2017BJ-35).

Declarations

Conflict of interest All authors declare that they have no conflict of interest.

Consent for publication All authors have agreed to submit the manuscript to Cellulose.

Ethical approval This article does not contain any studies with human participants or animals performed by any of the authors.

References

Ahmad AL, Low SC, Shukor SRA (2007) Effects of membrane cast thickness on controlling the macrovoid structure in lateral flow nitrocellulose membrane and determination of its characteristics. Scripta Mater 57:743–746. https://doi.org/10.1016/j.scriptamat.2007.06.037

Ahmad AL, Low SC, Shukor SRA, Ismail A (2008) Synthesis and characterization of polymeric nitrocellulose membranes: Influence of additives and pore formers on the membrane morphology. J Appl Polym Sci 108:2550–2557. https://doi.org/10.1002/app.27592

Alam N, Tong L, He Z, Tang R, Ahsan L, Ni Y (2021) Improving the sensitivity of cellulose fiber-based lateral flow assay by incorporating a water-dissolvable polyvinyl alcohol dam. Cellulose (lond) 28:8641–8651. https://doi.org/10.1007/s10570-021-04083-3

Bhardwaj J, Sharma A, Jang J (2019) Vertical flow-based paper immunosensor for rapid electrochemical and colorimetric detection of influenza virus using a different pore size sample pad. Biosens Bioelectron 126:36–43. https://doi.org/10.1016/j.bios.2018.10.008

Cao S, Ge W, Yang Y, Huang Q, Wang X (2021) High strength, flexible, and conductive graphene/polypropylene fiber paper fabricated via papermaking process. Adv Compos Hybrid Ma 5:104–112. https://doi.org/10.1007/s42114-021-00374-2

Charernchai S, Chikae M, Phan TT, Wonsawat W, Hirose D, Takamura Y (2022) Automated paper-based femtogram sensing device for competitive enzyme-linked immunosorbent assay of Aflatoxin B1 using submicroliter samples. Anal Chem 94:5099–5105. https://doi.org/10.1021/acs.analchem.1c05401

Chen R, Du X, Cui Y, Zhang X, Ge Q, Dong J, Zhao X (2020) Vertical flow assay for inflammatory biomarkers based on nanofluidic channel array and SERS nanotags. Small 16:e2002801. https://doi.org/10.1002/smll.202002801

Dignan LM, Woolf MS, Ross JA, Baehr C, Holstege CP, Pravetoni M, Landers JP (2021) A membrane-modulated centrifugal microdevice for enzyme-linked immunosorbent assay-based detection of lllicit and misused drugs. Anal Chem 93:16213–16221. https://doi.org/10.1021/acs.analchem.1c04102

Fan J, Zhang S, Li F, Yang Y, Du M (2020) Recent advances in cellulose-based membranes for their sensing applications. Cellulose (lond) 27:9157–9179. https://doi.org/10.1007/s10570-020-03445-7

Fernández de la Ossa MÁ, López-López M, Torre M, García-Ruiz C (2011) Analytical techniques in the study of highly-nitrated nitrocellulose. Trac-Trend Anal Chem 30:1740–1755. https://doi.org/10.1016/j.trac.2011.06.014

Gao B, Wang X, Li T, Feng Z, Wang C, Gu Z (2019a) Gecko-inspired paper artificial skin for intimate skin contact and multisensing. Adv Mater Technol-Us 4:1800392. https://doi.org/10.1002/admt.201800392

Gao Y, Zhu Z, Xi X, Cao T, Wen W, Zhang X, Wang S (2019b) An aptamer-based hook-effect-recognizable three-line lateral flow biosensor for rapid detection of thrombin. Biosens Bioelectron 133:177–182. https://doi.org/10.1016/j.bios.2019.03.036

Hartmann M, Kostrov X (2013) Immobilization of enzymes on porous silicas-benefits and challenges. Chem Soc Rev 42:6277–6289. https://doi.org/10.1039/c3cs60021a

Horstmann B, okoyama KY, Avrutin ÜÖaV, (2020) Electrically induced decomposition of thin-film nitrocellulose membranes for on-demand biosensor activation. 2020 SoutheastCon. https://doi.org/10.1109/southeastcon44009.2020.9249726

Hu J, Wang L, Li F, Han YL, Lin M, Lu TJ, Xu F (2013) Oligonucleotide-linked gold nanoparticle aggregates for enhanced sensitivity in lateral flow assays. Lab Chip 13:4352–4357. https://doi.org/10.1039/c3lc50672j

Huang Q, Yang Y, Chen R, Wang X (2021) High performance fully paper-based all-solid-state supercapacitor fabricated by a papermaking process with silver nanoparticles and reduced graphene oxide-modified pulp fibers. EcoMat 3:e12076. https://doi.org/10.1002/eom2.12076

Ince B, Sezginturk MK (2022) Lateral flow assays for viruses diagnosis: up-to-date technology and future prospects. Trac-Trend Anal Chem 157:116725. https://doi.org/10.1016/j.trac.2022.116725

Khamis MF, Low SC (2020) Thermal mechanical stretching to imprint pores morphology of nitrocellulose membrane for immuno-sensing application. J Appl Membr Sci Technol 24:67–79. https://doi.org/10.11113/amst.v24n1.178

Li Y, Tran L, Filipe CDM, Brennan JD, Pelton RH (2019) Printed thin films with controlled porosity as lateral flow media. Ind Eng Chem Res 58:21014–21021. https://doi.org/10.1021/acs.iecr.9b02177

Liao C, Mu X, Han L, Li Z, Zhu Y et al (2022) A flame-retardant, high ionic-conductivity and eco-friendly separator prepared by papermaking method for high-performance and superior safety lithium-ion batteries. Energy Storage Mater 48:123–132. https://doi.org/10.1016/j.ensm.2022.03.008

Lin D, Li B, Fu L, Qi J, Xia C et al (2022) A novel polymer-based nitrocellulose platform for implementing a multiplexed microfluidic paper-based enzyme-linked immunosorbent assay. Microsyst Nanoeng 8:53. https://doi.org/10.1038/s41378-022-00385-z

Liu P, Fu L, Song Z, Man M, Yuan H et al (2021a) Three dimensionally printed nitrocellulose-based microfluidic platform for investigating the effect of oxygen gradient on cells. Analyst 146:5255–5263. https://doi.org/10.1039/d1an00927c

Liu Y, Zhan L, Qin Z, Sackrison J, Bischof JC (2021b) Ultrasensitive and highly specific lateral flow assays for point-of-care diagnosis. ACS Nano 15:3593–3611. https://doi.org/10.1021/acsnano.0c10035

Liu Y, Zhang S, Li L, Coseri S (2023) Cellulose nanofiber extraction from unbleached kraft pulp for paper strengthening. Cellulose 30:3219–3235. https://doi.org/10.1007/s10570-022-05008-4

Low SC, Shaimi R, Thandaithabany Y, Lim JK, Ahmad AL, Ismail A (2013) Electrophoretic interactions between nitrocellulose membranes and proteins: biointerface analysis and protein adhesion properties. Colloid Surf B 110:248–253. https://doi.org/10.1016/j.colsurfb.2013.05.001

Luo Y, Nartker S, Wiederoder M, Miller H, Hochhalter D, Drzal LT, Alocilja EC (2012) Novel biosensor based on electrospun nanofiber and magnetic nanoparticles for the detection of E. coli O157:H7. Ieee T Nanotechnol 11:676–681. https://doi.org/10.1109/tnano.2011.2174801

Modha S, Castro C, Tsutsui H (2021) Recent developments in flow modeling and fluid control for paper-based microfluidic biosensors. Biosens Bioelectron 178:113026. https://doi.org/10.1016/j.bios.2021.113026

Naderizadeh B, Moghimi A, Shahi M (2012) Electrospun nitrocellulose and composite nanofibers. J Nanostruct 2:287–293. https://doi.org/10.7508/JNS.2012.03.003

Noviana E, Ozer T, Carrell CS, Link JS, McMahon C, Jang I, Henry CS (2021) Microfluidic paper-based analytical devices: from design to applications. Chem Rev 121:11835–11885. https://doi.org/10.1021/acs.chemrev.0c01335

Pawar VM, Nadkarni VS (2019) Preparation of thin films of cellulose acetate-nitrocellulose blend for solid state nuclear track detection using spin coating technique. J Radioanal Nucl Ch 323:1329–1338. https://doi.org/10.1007/s10967-019-06931-w

Sathirapongsasuti N, Panaksri A, Boonyagul S, Chutipongtanate S, Tanadchangsaeng N (2021) Electrospun fibers of polybutylene succinate/graphene oxide composite for syringe-push protein absorption membrane. Polymers-Basel 13:2042. https://doi.org/10.3390/polym13132042

Sebe G, Ham-Pichavant F, Ibarboure E, Koffi AL, Tingaut P (2012) Supramolecular structure characterization of cellulose II nanowhiskers produced by acid hydrolysis of cellulose I substrates. Biomacromol 13:570–578. https://doi.org/10.1021/bm201777j

Seki Y, Selli F, Erdoğan ÜH, Atagür M, Seydibeyoğlu MÖ (2022) A review on alternative raw materials for sustainable production: novel plant fibers. Cellulose 29:4877–4918. https://doi.org/10.1007/s10570-022-04597-4

Sena-Torralba A, Alvarez-Diduk R, Parolo C, Piper A, Merkoci A (2022) Toward next generation lateral flow assays: integration of nanomaterials. Chem Rev 122:14881–14910. https://doi.org/10.1021/acs.chemrev.1c01012

Sun H, Liu S, Ge B, Xing L, Chen H (2007) Cellulose nitrate membrane formation via phase separation induced by penetration of nonsolvent from vapor phase. J Membrane Sci 295:2–10. https://doi.org/10.1016/j.memsci.2007.02.019

Sun H, Liu Y, Guo X, Zeng K, Kanti Mondal A et al (2021) Strong, robust cellulose composite film for efficient light management in energy efficient building. Chem Eng J 425:131469. https://doi.org/10.1016/j.cej.2021.131469

Tang R, Yang H, Choi JR, Gong Y, Hu J et al (2016) Improved sensitivity of lateral flow assay using paper-based sample concentration technique. Talanta 152:269–276. https://doi.org/10.1016/j.talanta.2016.02.017

Tang RH, Liu LN, Zhang SF, He XC, Li XJ et al (2019a) A review on advances in methods for modification of paper supports for use in point-of-care testing. Microchim Acta 186:521. https://doi.org/10.1007/s00604-019-3626-z

Tang RH, Li M, Liu LN, Zhang SF, Alam N et al (2020) Chitosan-modified nitrocellulose membrane for paper-based point-of-care testing. Cellulose 27:3835–3846. https://doi.org/10.1007/s10570-020-03031-x

Tang R, Li M, Yan X, Liu LN, Li Z, Xu F (2022a) Comparison of paper-based nucleic acid extraction materials for point-of-care testing applications. Cellulose 29:2479–2495. https://doi.org/10.1007/s10570-022-04444-6

Tang Y, Xing L, Wang P (2019b) Preparation of a hydrophilic nitrocellulose membrane. IOP Conf Ser: Mater Sci Eng 677:022035. https://doi.org/10.1088/1757-899x/677/2/022035

Tang R, Alam N, Li M, Xie M, Ni Y (2021) Dissolvable sugar barriers to enhance the sensitivity of nitrocellulose membrane lateral flow assay for COVID-19 nucleic acid. Carbohydr Polym 268:118259. https://doi.org/10.1016/j.carbpol.2021.118259

Tang R, Xie MY, Li M, Cao L, Feng S, Li Z, Xu F (2022b) Nitrocellulose membrane for paper-based biosensor. Appl Mater Today 26:101305. https://doi.org/10.1016/j.apmt.2021.101305

Trache D, Khimeche K, Mezroua A, Benziane M (2016) Physicochemical properties of microcrystalline nitrocellulose from Alfa grass fibres and its thermal stability. J Therm Anal Calorim 124:1485–1496. https://doi.org/10.1007/s10973-016-5293-1

Wang X, Yang D, Jia ST, Zhao LL, Jia TT, Xue CH (2020) Electrospun nitrocellulose membrane for immunochromatographic test strip with high sensitivity. Microchim Acta 187:644. https://doi.org/10.1007/s00604-020-04626-8

Wang X, Xue CH, Yang D, Jia ST, Ding YR et al (2021) Modification of a nitrocellulose membrane with nanofibers for sensitivity enhancement in lateral flow test strips. RSC Adv 11:26493–26501. https://doi.org/10.1039/d1ra04369b

Wang C, Wu R, Ling H, Zhao Z, Han W et al (2022a) Toward scalable fabrication of electrochemical paper sensor without surface functionalization. Npj Flex Electron 6:1–8. https://doi.org/10.1038/s41528-022-00143-1

Wang Y, Wan Y, Li S, Guo L (2022b) Facile fabrication of metastable aluminum/fluoropolymer composite films by spin-coating and their thermal properties. J Polym Res 29:108593. https://doi.org/10.1007/s10965-022-02934-6

Xiao M, Tian F, Liu X, Zhou Q, Pan J et al (2022) Virus detection: from state-of-the-art laboratories to

smartphone-based point-of-care testing. Adv Sci 9:2105904–2105929. https://doi.org/10.1002/advs.202105904

Yahaya ML, Zakaria ND, Noordin R, Razak KA (2019) The effect of nitrocellulose membrane pore size of lateral flow immunoassay on sensitivity for detection of Shigella sp. in milk sample. Mater Today: Proc 17:878–883. https://doi.org/10.1016/j.matpr.2019.06.384

Yew CT, Azari P, Choi JR, Li F, Pingguan-Murphy B (2018) Electrospin-coating of nitrocellulose membrane enhances sensitivity in nucleic acid-based lateral flow assay. Anal Chim Acta 1009:81–88. https://doi.org/10.1016/j.aca.2018.01.016

Yin L-T, Lin Y-T, Leu Y-C, Hu C-Y (2010) Enzyme immobilization on nitrocellulose film for pH-EGFET type biosensors. Sensor Actuat B-Chem 148:207–213. https://doi.org/10.1016/j.snb.2010.04.042

Zhang S-F, Liu L-N, Tang R-H, Liu Z, He X-C, Qu Z-G, Li F (2019) Sensitivity enhancement of lateral flow assay by embedding cotton threads in paper. Cellulose 26:8087–8099. https://doi.org/10.1007/s10570-019-02677-6

Zheng S, Yang X, Zhang B, Cheng S, Han H et al (2021) Sensitive detection of Escherichia coli O157:H7 and Salmonella typhimurium in food samples using two-channel fluorescence lateral flow assay with liquid Si@ quantum dot. Food Chem 363:130400. https://doi.org/10.1016/j.foodchem.2021.130400

Zhu C, Zhang J, Xu J, Yin X, Wu J et al (2019) Aramid nanofibers/polyphenylene sulfide nonwoven composite separator fabricated through a facile papermaking method for lithium ion battery. J Membr Sci 588:117169. https://doi.org/10.1016/j.memsci.2019.117169